LIP-STUDENTS-25-10

Modelling Atomic Signatures of Heavy Elements in kilonovae

Francisco Rosendo[1,a]

[1] *Faculdade de Ciências da Universidade de Lisboa*

Project supervisors: Ricardo Ferreira da Silva, Luis Leitão, Jorge Sampaio, Daniel Garcia

September 30, 2025

Abstract. The first direct observation of a kilonova (AT2017gfo) associated with gravitational wave event GW170817 in 2017, and the subsequent detection of AT2023vfi, have provided unprecedented opportunities to study r-process nucleosynthesis in neutron star mergers. Spectroscopic analysis of these events suggests the presence of heavy elements, but definitively identifying specific elements requires accurate atomic data and robust spectral modeling. This work will be focused on forbidden transitions of elements like tungsten (W), platinum (Pt), gold (Au), and lanthanides, particularly in the near and mid-infrared wavelength regions where telescopes like the James Webb Space Telescope (JWST) offers enhanced observational capabilities.

Keywords: kilonovae, supernovae, spectra, neuron star merger, LTE, NLTE, r-process

1 Introduction

Elements up to the iron peak are predominantly synthesized via stellar nucleosynthesis. The r-process is responsible for producing heavier elements and it's believed these can be found in extreme events, some have been found in spectra coming from exploding stars, called supernovae. But, as seen in figure 1, some are believed to come from more extreme events, such as neutron star mergers. When neutron stars collide or when a neutron star collides with a black hole, the electromagnetic radiation emitted in the explosion is called a kilonova. [1] [2]

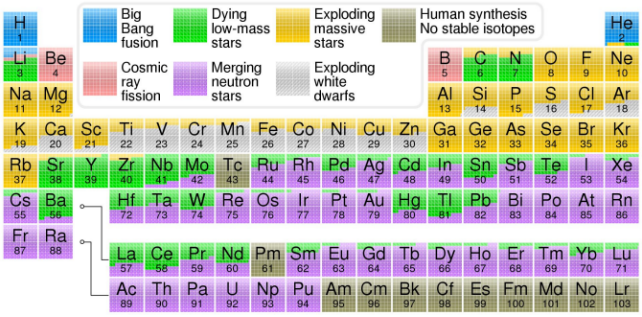

Figure 1. Periodic table showcasing the sites of nucleosynthesis Credit: Wikipedia user Cmglee, image created based on data from [3].

The purpose of this work was to develop a model that will find atomic signatures for these heavier elements.

As it can be seen in figure 2 , kilonovae spectra show very broad features, with a high density of lines that make it hard to pinpoint specific features of a single ion. For this reason, and since these events are rare and not very well known, the model was benchmarked with a supernova spectrum as these are well known and more common events and the goal is to validate the model's implementation of physics using a high-quality public dataset with much clearer features. [5] [6] [7]

[a] e-mail: fx.rosendo@gmail.com

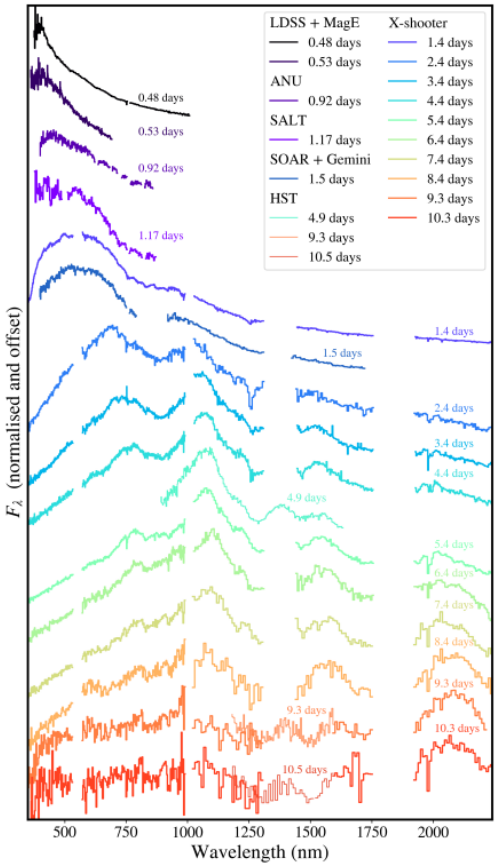

Figure 2. Spectrum of a kilonova from [4].

The model was benchmarked with the spectrum of Type Ia supernova Sn 2011fe as seen in 5, in appendix A, with the information published in [8] and downloaded from [9].

2 Method

Local Thermodynamic Equilibrium (LTE) assumes collisions between particles are so frequent that they dominate all other processes. The gas has enough time to settle into

a thermal equilibrium locally. In LTE ionization follows the Saha equation, relative level population is described by the Boltzmann equation and emission follows the Planck Function.

2.1 Spectrum Analysis

The method started by analysing the spectrum to register at which wavelengths absorption lines can be found. This was done by finding the local minima in the flux with `find_peaks` function from *Python*'s library `scipy.signal`, the lines' properties such as width and depth were also acquired. These method has faults such as dealing with noise in the data and distinguish blended lines. The lines that were found can be seen in figure 6, in appendix A.

The same function was used to find the flux's peak and calculate the object's temperature using Wien's displacement law.

$$\lambda_{\text{peak}}\, T = b_{\text{W}} \tag{1}$$

Where λ_{peak} is the wavelength at which the flux is highest, T is the temperature and b_W is the constant of value 2.898×10^{-3} m K. This temperature was used to get the Planck function for the supernova's temperature, which was normalized and will be used for the modelling. All of this can be seen in figure 7, in appendix A.

$$B_\lambda(\lambda, T) = \frac{2hc^2}{\lambda^5} \frac{1}{e^{hc/(\lambda k_B T)} - 1} \tag{2}$$

B_λ is the body's spectral radiance, λ is the wavelength, h is the Planck's constant, c is the speed of light in a vacuum and k_{B} is the Boltzmann's constant.

2.2 Atomic Populations

After analysing the spectrum, atomic populations were calculated assuming LTE and using line and ionization energy data from National Institute of Standards and Technology (NIST) Atomic Spectra Database (ASD) [10] and atomic weight data from NIST Database [11]. Only data from elements up to Fe was used. [12]

2.2.1 Relative Level Population - Boltzmann Equation

The fraction in each element's level follows the Bolztamnn distribution.

$$\frac{n_{\text{i}}^*}{n_{\text{j}}^*} = \frac{g_{\text{i}}}{g_{\text{j}}} \exp\left(-\Delta E_{\text{ij}}/k_{\text{B}}T\right) \tag{3}$$

n_i^* being an atomic level, g_i its degeneracy and $\Delta E_{\text{ij}} = E_{\text{j}} - E_{\text{i}}$ where E_{i} is the energy of the level.

To get the fraction relative to all available levels the partition function, U_{zk}, and the total population of the ionisation stage, N_{zk}^*, are needed:

$$U_{\text{zk}} = \sum_{\text{i}=0}^{\infty} g_{\text{i}} \exp\left(-\Delta E_{\text{i0}}/k_{\text{B}}T\right) \tag{4}$$

where 0 denotes the ground state.

$$N_{\text{zk}}^* = \frac{n_0}{g_0} U_{zk} \tag{5}$$

Equation 6 can then be gotten from equations 3, 4 and 5.

$$\frac{n_{\text{i}}^*}{N_{\text{zk}}^*} = \frac{g_{\text{i}}\, \exp\left(-\Delta E_{\text{ij}}/k_{\text{B}}T\right)}{U_{\text{zk}}} \tag{6}$$

As an example, the plot shown in figure 3 shows the Boltzmann equation applied to the first 10 levels of neutral Carbon (C I) for different temperatures.

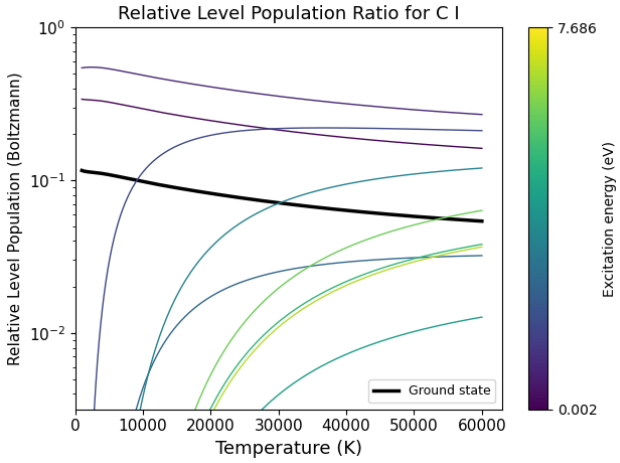

Figure 3. Relative level population versus temperature for the first ten levels of neutral Carbon. Calculated with the Botzmann equation.

2.2.2 Relative Ion Population - Saha Equation

The fraction in each element's ionization state is governed by the Saha Equation (equation 7)

$$\frac{N_{\text{z+1,k}}}{N_{\text{z,k}}} = \frac{2U_{\text{z+1,k}}}{N_{\text{e}} U_{\text{zk}}} \left(\frac{2\pi m_{\text{e}} k_{\text{B}} T}{h^2}\right)^{3/2} \exp\left(-\chi_{\text{z}}/k_{\text{B}}T\right) \tag{7}$$

Where $N_{z,k}$ is the distribution of atoms over ionisation stage z, N_e is the electron density, m_e the electron mass and χ_z the ionisation energy of the atom in ionisation state z.

Equation 7 only gives the fraction of an ionization state compared to another, therefore equation 8 has to be used to get the fraction relative to all possible ionization states.

$$\begin{aligned} \frac{N_0}{N_k} &= \frac{N_0}{N_0 + N_1 + N_2 + \ldots} \\ &= \frac{1}{1 + \frac{N_1}{N_0} + \frac{N_2}{N_0} + \ldots} \\ &= \frac{1}{1 + \frac{N_1}{N_0} + \frac{N_2}{N_1}\frac{N_1}{N_0} + \ldots} \end{aligned} \tag{8}$$

The plot shown in figure 4 shows the Saha equation applied to all Carbon (C) ionization stages for different temperatures as an example.

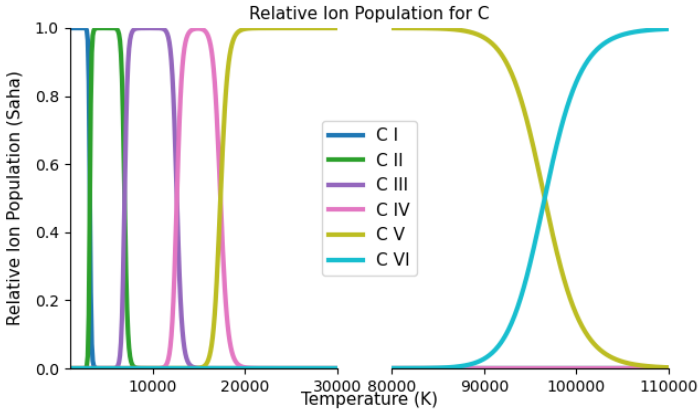

Figure 4. Relative ionization state versus temperature for all Carbon ionization states. Calculated with the Saha equation.

2.3 Opacity and Modelling

The Sobolev Optical Depth describes how much light is absorbed by a given line and it can be calculated with these values as well as some of the lines' physical properties through equation 9.

$$\tau_{\mathrm{lu}} = \frac{\pi e^2}{m_{\mathrm{e}} c} f_{\mathrm{lu}} n_{\mathrm{l}} \lambda_0 t \tag{9}$$

Where e is the electron's charge, f_{lu} describes the line's intrinsic strength, t is the specific time after the explosion at which the spectrum was taken. n_{l} is the number of absorbers, it's the result of the product between the Ionization Fraction (equation 8), the Level Population Fraction (equation 6) and the Total Number Density of the Element. The Total Number Density of the Element is given by $\rho \times \frac{N_A}{M}$, with ρ being the supernova´s density, N_A the Avogadro number and M the element's Relative Atomic Mass.

For the modelling the Radiative Transfer Equation, 10, needs to be solved.

$$\frac{d\, I_\nu}{d\, s} = j_\nu - \alpha_\nu I_\nu \tag{10}$$

The photospheric approximation assumes the supernova's photosphere is the only source of light, ignoring any emission from the gas ($j_\nu = 0$) and that the final spectrum is the initial continuum attenuated by the absorption from all intervening gas, intensity will be given by:

$$I_\lambda = B_\lambda(T)\, e^{-\tau_\lambda} \tag{11}$$

NIST's ASD's line data was used to find which elements' lines could be found within the spectrum's absorption lines, using their width as wavelength tolerance. figure 8, in appendix A, was obtained by applying 11 with these lines.

Figure 8 has some issues however, two of them being that it assumes all elements found in this supernova are equally abundant and only showing the lines that were found. To fix the first issue solar photosphere abundances were used as a test [13]. This isn't entirely correct, and a proper benchmark would require an abundance set dominated by iron-group elements which was harder to achieve. The second issue was fixed by adding all the lines for the elements present in the plot, this means if Fe II were found in an absorption line then all other Fe II lines would be added, obtaining the plot shown in figure 9, in appendix A.

2.4 Line Broadening

In reality, absorption lines should not be as sharp as seen in 9 as there are several effects broadening the lines such as natural, doppler, collisional broadening and broadening coming from the expansion of the photosphere.

Two of these broadening terms were then introduced; Thermal doppler broadening and the expansional broadening. Thermal doppler broadening happens due to the random, microscopic thermal motion of individual atoms and creates a Gaussian line profile. Expansional broadening also as a Gaussian profile and it comes from the motion of the absorbing material in an expanding system.

2.5 Interactive Plot

As the lines were broadened the plots became overly dense and difficult to interpret due to the high number of overlapping lines so an interactive plot was made to carefully select only the elements that the user would want to see. As the abundances used were only a test, an abundance slider was incorporated in the interactive plot to adjust these values. Along with it a redshift and expansion velocity sliders were also incorporated. This can be showcased in 10, where ionized silicon (Si II) was selected.

3 Conclusions and Future work

As this model is meant to be applied to kilonovae spectra, the next step would be to implement Non-Local Thermodynamic Equilibrium (NLTE) as this is a better approximation for kilonovae. This is due to the low densities and rapid expansion of the ejecta, which prevent the plasma from reaching a collisional equilibrium. NLTE is a state where collisions are infrequent and the radiation from the photosphere becomes the driving mechanism for atomic processes.

The other broadening effects should also be added despite their minimal effect on the broadening of the lines.

It would also be wise to have a χ^2 or any other type of statistical test on the interactive plot to showcase how accurately a certain element fits in the spectrum as the user uses the sliders, this could then be useful to implement machine learning to adjust these for each element and get the perfect fit. There are also some upgrades that could be done not only to the way these sliders work but to the rest of the code itself for performance and readability.

Acknowledgements

I would like to thank LIP for the opportunity and everyone at NUC-RIA for the help they provided, my supervisors, both official and unofficial, and the other interns I met, who either had direct or indirect contact with the outcome of this work. I would like to thank everyone who helped me with this project, everyone who taught me about this new subject and anyone who suggested ideas or implementations in any way, that I may or may not have been able to implement in the final product.

References

[1] Brian D Metzger, G Martínez-Pinedo, S Darbha, E Quataert, Almudena Arcones, D Kasen, R Thomas, P Nugent, IV Panov, and Nikolaj Thomas Zinner. Electromagnetic counterparts of compact object mergers powered by the radioactive decay of r-process nuclei. *Monthly Notices of the Royal Astronomical Society*, 406(4):2650–2662, 2010.

[2] AstroSat Cadmium Zinc Telluride Imager Team, AGILE Team, The Team, The Dark Energy Camera GW Collaboration, GRAvitational Wave Inaf TeAm, Australian SKA Pathfinder, Las Cumbres Observatory Group, CAASTRO Collaborations, Caltech NRAO, NuSTAR Collaborations, et al. Multi-messenger observations of a binary neutron star merger. *arXiv preprint arXiv:1710.05833*, 2017.

[3] Jennifer A Johnson, Gail Zasowski, David Weinberg, Yuan-Sen Ting, Jennifer Sobeck, Verne Smith, Victor Silva Aguirre, David Nataf, Sara Lucatello, Juna Kollmeier, et al. The Origin of Elements Across Cosmic Time: Astro2020 Science White Paper. *arXiv preprint arXiv:1907.04388*, 2019.

[4] Albert Sneppen, Darach Watson, Rasmus Damgaard, Kasper E Heintz, Nicholas Vieira, Petri Väisänen, and Antoine Mahoro. Emergence hour-by-hour of r-process features in the kilonova at2017gfo. *Astronomy & Astrophysics*, 690:A398, 2024.

[5] Daniel Kasen, Brian Metzger, Jennifer Barnes, Eliot Quataert, and Enrico Ramirez-Ruiz. Origin of the heavy elements in binary neutron-star mergers from a gravitational-wave event. *Nature*, 551(7678):80–84, 2017.

[6] Masaomi Tanaka, Daiji Kato, Gediminas Gaigalas, and Kyohei Kawaguchi. Systematic opacity calculations for kilonovae. *Monthly Notices of the Royal Astronomical Society*, 496(2):1369–1392, 2020.

[7] Andreas Flörs, Ricardo F Silva, Jerome Deprince, Helena Carvajal Gallego, G Leck, LJ Shingles, Gabriel Martínez-Pinedo, JM Sampaio, P Amaro, JP Marques, et al. Opacities of singly and doubly ionized neodymium and uranium for kilonova emission modeling. *Monthly Notices of the Royal Astronomical Society*, 524(2):3083–3101, 2023.

[8] Benjamin E Stahl, WeiKang Zheng, Thomas De Jaeger, Thomas G Brink, Alexei V Filippenko, Jeffrey M Silverman, S Bradley Cenko, Kelsey I Clubb, Melissa L Graham, Goni Halevi, et al. Berkeley supernova ia program: data release of 637 spectra from 247 type ia supernovae. *Monthly Notices of the Royal Astronomical Society*, 492(3):4325–4343, 2020.

[9] Ofer Yaron and Avishay Gal-Yam. Wiserep—an interactive supernova data repository. *Publications of the Astronomical Society of the Pacific*, 124(917):668, 2012. Available online on https://wiserep.org/.

[10] A. Kramida, Yu. Ralchenko, J. Reader, and NIST ASD Team. NIST Atomic Spectra Database (version 5.12). Online, https://physics.nist.gov/asd, 2024. Accessed 2025-09-22.

[11] Schwab D.J. Tsai J.J. Coursey, J.S. and R.A. Dragoset. Atomic Weights and Isotopic Compositions (version 4.1). [Online] Available: http://physics.nist.gov/Comp, 2015. Accessed 2025-09-22.

[12] ALAN P. RYBICKI, GEORGE B.. LIGHTMAN. *Radiative processes in astrophysics*. WILEY-VCH, 2024.

[13] Katharina Lodders. Solar elemental abundances. *arXiv preprint arXiv:1912.00844*, 2019.

A Supporting images

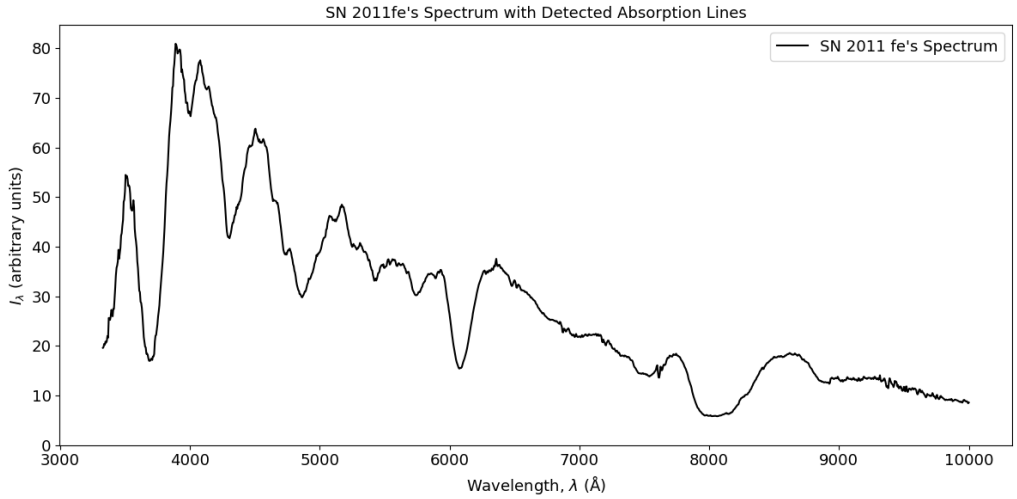

Figure 5. Spectrum of SN 2011fe.

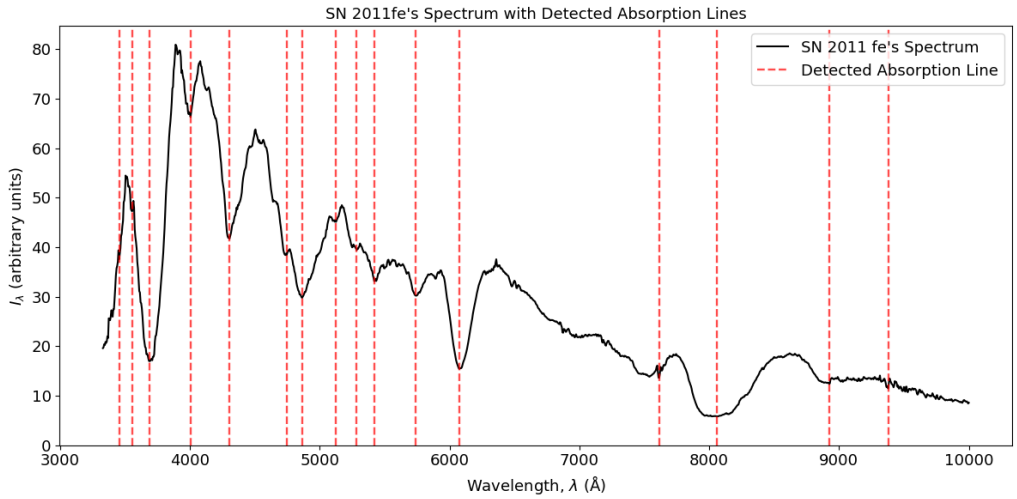

Figure 6. Spectrum of SN 2011fe showcasing the detected absorption lines.

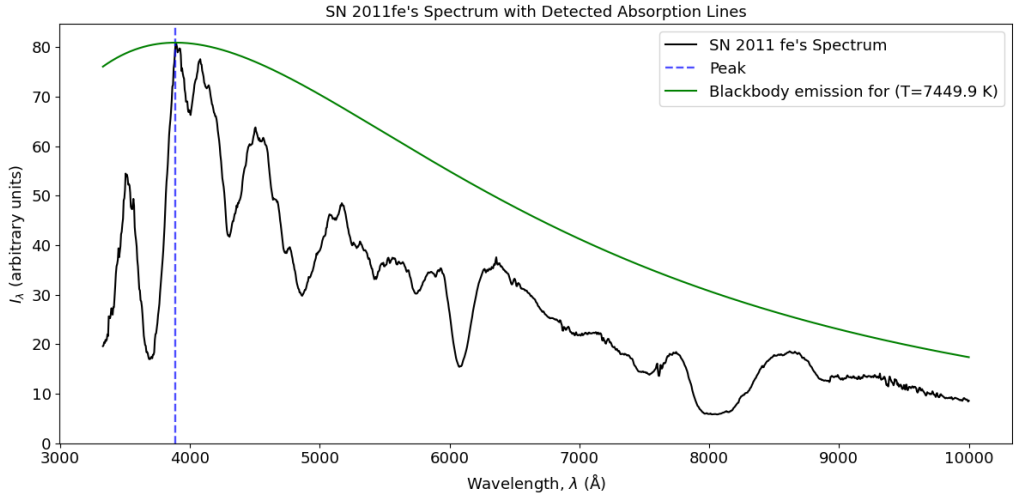

Figure 7. Spectrum of SN 2011fe showcasing the peak of the flux and the Planck Function.

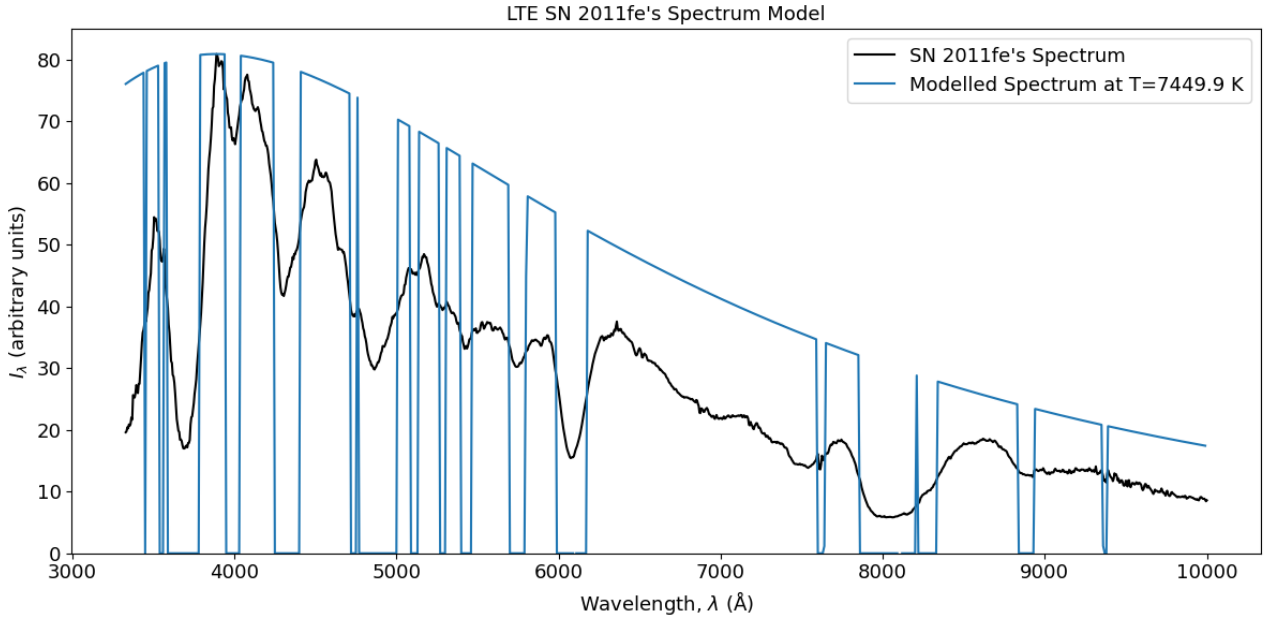

Figure 8. Spectrum of SN 2011fe and the modelled version of the Spectrum. In this model the elements found are treated as if they were equally abundant and only lines found by the model are taken into account.

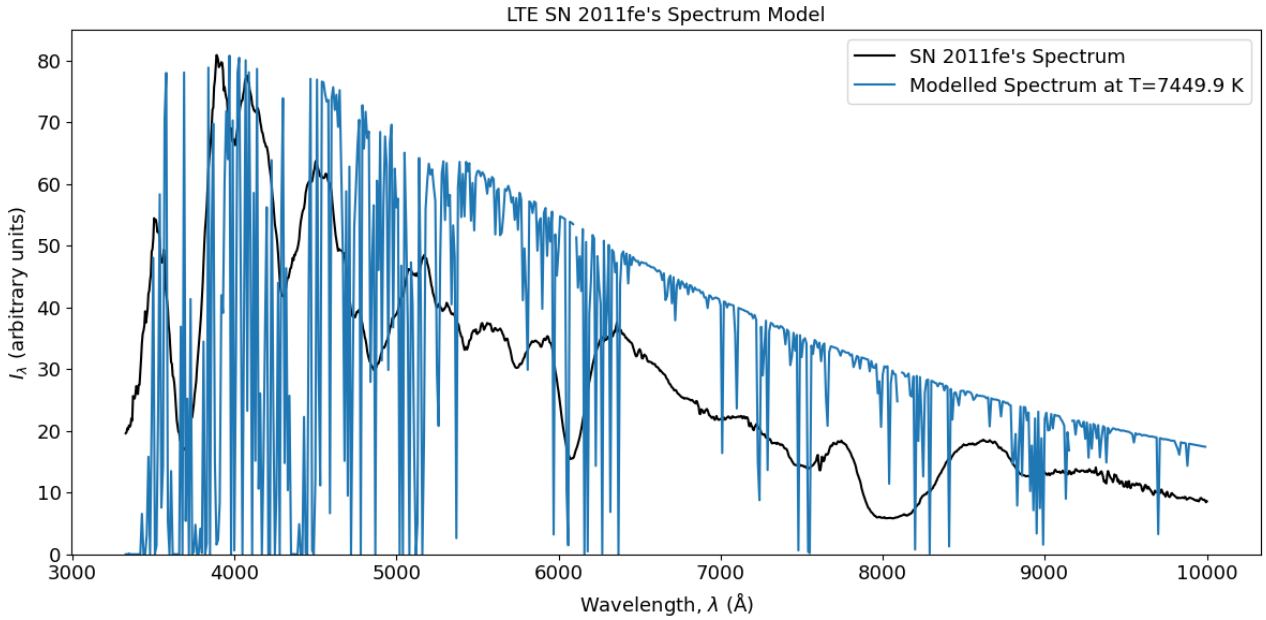

Figure 9. Spectrum of SN 2011fe and the modelled version of the Spectrum. In this model solar photosphere abundances were used and all the lines for found ions were added.

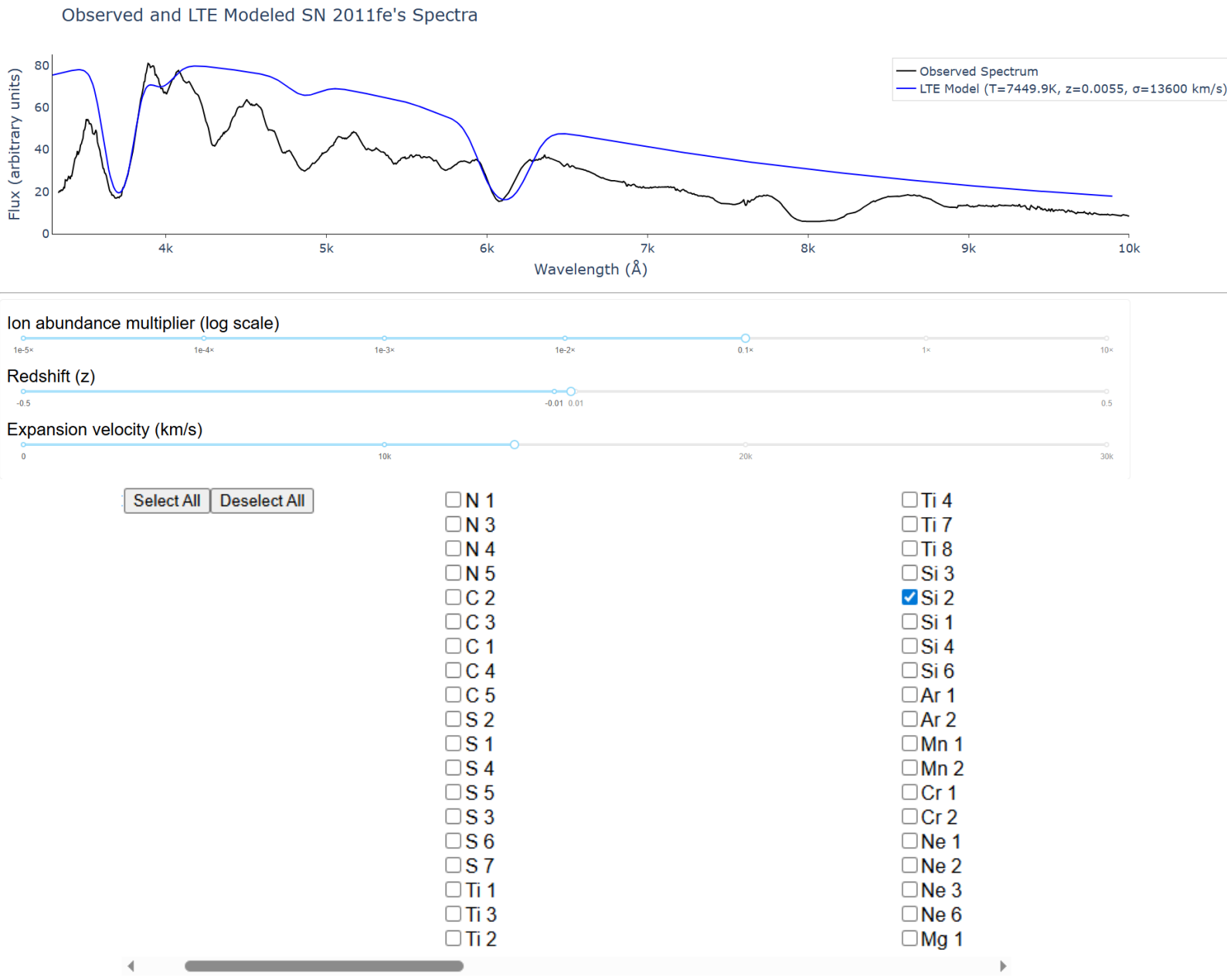

Figure 10. Interactive plot showing the model applied to ionized silicon. The sliders have been tweaked to fit the model.